

Article

## Acceleration Slip Regulation Strategy for Distributed Drive Electric Vehicles with Independent Front Axle Drive Motors

Lingfei Wu <sup>1,2</sup>, Jinfang Gou <sup>1</sup>, Lifang Wang <sup>1,\*</sup> and Junzhi Zhang <sup>3</sup>

<sup>1</sup> Key Laboratory of Power Electronics and Electric Drive, Institute of Electrical Engineering, Chinese Academy of Sciences, Beijing 100190, China;

E-Mails: wulingfei10@mails.ucas.ac.cn (L.W.); goujinfang@mail.iee.ac.cn (J.G.)

<sup>2</sup> University of Chinese Academy of Sciences, Beijing 100049, China

<sup>3</sup> State Key Laboratory of Automotive Safety and Energy, Tsinghua University, Beijing 100084, China; E-Mail: jzhzhang@mail.tsinghua.edu.cn

\* Author to whom correspondence should be addressed; E-Mail: wlf@mail.iee.ac.cn; Tel.: +86-10-6279-5610 (ext. 123); Fax: +86-10-6277-1839.

Academic Editor: Omar Hegazy

Received: 31 December 2014 / Accepted: 23 April 2015 / Published: 8 May 2015

---

**Abstract:** This paper presents an acceleration slip regulation strategy for distributed drive electric vehicles with two motors on the front axle. The tasks of the strategy include controlling the slip ratio to make full use of the road grip and controlling the yaw rate to eliminate the lateral movement due to the difference between motor torques. The rate of the slip ratio change can be controlled by controlling the motor torque, so that the slip ratio can be controlled by applying a proportional-integral control strategy to control the rate of the slip ratio change. The yaw rate can be controlled to almost zero by applying torque compensation based on yaw rate feedback. A coordination control strategy for the slip ratio control and yaw rate control is proposed based on analysis of the priorities and features of the two control processes. Simulations were carried out using MATLAB/Simulink, and experiments were performed on a hardware-in-loop test bench with actual motors. The results of the simulations and experiments showed that the proposed strategy could improve the longitudinal driving performance and straight line driving stability of the vehicle.

**Keywords:** acceleration slip regulation; distributed drive electric vehicle; slip ratio control; yaw rate control

---

## 1. Introduction

Because of the growing public concern about the global environmental and energy problems, electric vehicles have become a hot research topic. Significant improvements in power electronics and power and control strategies have been achieved, which have promoted the development of electric vehicles [1,2]. As a new research area for electric vehicles, the distributed drive electric vehicle, which employs motors to drive the wheels independently, is drawing increasing attention because of its advantages, which include a flexible chassis layout, quick torque response, easy measurements, and vehicle dynamic control with multiple degrees of control freedom due to the independent wheel torque control [3–5].

Acceleration slip regulation is an important aspect of vehicle dynamic control. It can help to prevent excessive wheel spin and to make full use of the road grip when the driver torque command exceeds the maximum torque provided by the road. Compared to conventional vehicles, the sensitive torque response and accurate torque control make the acceleration slip regulation of the electric vehicle faster and more accurate. Most acceleration slip regulation methods are based on slip ratio control. This method requires the vehicle speed, which can be obtained using the speed of the driven wheels or vehicle speed sensors. A traditional logic threshold control strategy for the acceleration slip regulation of an electric vehicle has been proposed [6,7]. In addition, common control methods like proportional-integral-derivative (PID) control, sliding mode control, and fuzzy control can also be used to realize acceleration slip control [8–12]. Using information from the motor, scholars have found other methods that do not require the vehicle speed. These methods are mainly based on the wheel speed and wheel acceleration. Model following control and maximum transmissible torque estimation are also feasible methods for acceleration slip regulation control [3,13–15]. For a distributed drive electric vehicle, the acceleration slip regulation control can be applied to independent wheels, where the motors are considered to be the same. When the driving wheels on the same axle are under different road conditions, the higher wheel rotational speed will be used as the reference wheel speed [16]. However, these methods would be affected by the nonlinearity of the system and the error in the actual motor torque output. Furthermore, for a distributed drive electric vehicle, the difference between the motor torques on the same axle due to the motor characteristics will affect the straight line driving stability of the vehicle.

This paper presents an acceleration slip regulation strategy that combines slip ratio control and yaw rate control. The slip ratio control aims at making full use of the road adhesion, while the yaw rate control aims at keeping the vehicle running in a straight line. A simulation model for a distributed drive electric vehicle with two independent drive motors near the wheels on the front axle was constructed using MATLAB/Simulink, and simulations were performed. Experiments were also conducted on a hardware-in-loop test bench with actual vehicle motors.

## 2. System Model

In this study, a simulation model of a distributed drive electric vehicle was constructed using MATLAB/Simulink. The vehicle is driven by two independently controlled motors mounted close to the wheels on the front axle and powered by a battery placed in the trunk of the vehicle. The chassis

layout of the vehicle is shown in Figure 1. The parameters of the vehicle are based on an experimental electric vehicle. The main parameters of the model are listed in Table 1.

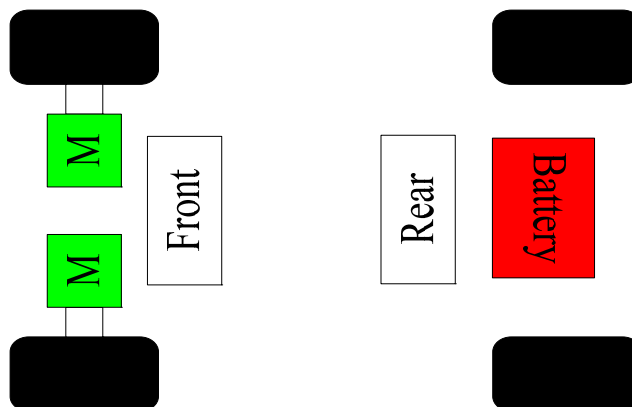


Figure 1. Chassis layout of vehicle model.

Table 1. Main parameters of vehicle.

Parameter	Value
Vehicle mass	1,500 kg
Driving axle	front
Number of motors	2
Motor Power	20 kW
Maximum speed	8,000 r/min
Gear ratio	7.8

2.1. Vehicle Dynamic Model

In order to analyze the longitudinal and yawing motions, a vehicle dynamic model with eight degrees of freedom was constructed using MATLAB/Simulink. The longitudinal motion, lateral motion, yawing motion of the chassis, steering angle of the front wheels, and rotational motion of the wheels were taken into consideration. The vehicle dynamic model is shown in Figure 2.

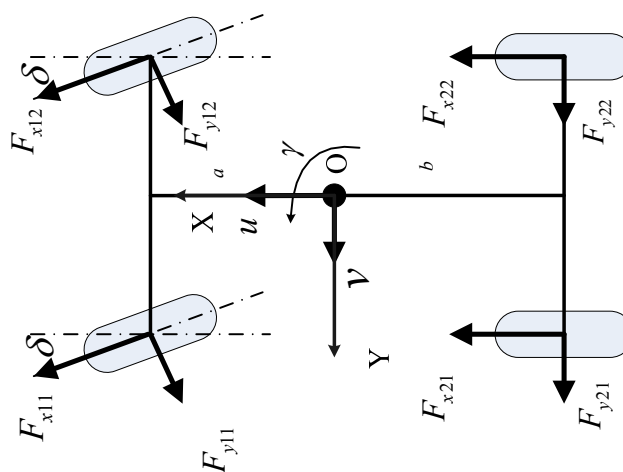


Figure 2. Vehicle dynamic model.

The motion of the vehicle chassis includes the longitudinal, lateral, and yawing motions. The motion equations can be described as follows [17]:

$$\begin{cases} m(\dot{u} - v\gamma) = (F_{x11} + F_{x12}) \cos \delta - (F_{y11} + F_{y12}) \sin \delta + F_{x21} + F_{x22} - F_w \\ m(\dot{v} + u\gamma) = (F_{x11} + F_{x12}) \sin \delta + (F_{y11} + F_{y12}) \cos \delta + F_{y21} + F_{y22} \\ I\dot{\gamma} = \frac{B}{2}[(F_{x12} - F_{x11}) \cos \delta + (F_{y11} - F_{y12}) \sin \delta] + \frac{B}{2}(F_{x22} - F_{x21}) \\ + a[(F_{x12} + F_{x11}) \sin \delta + (F_{y12} + F_{y11}) \cos \delta] - b(F_{y22} + F_{y21}) \end{cases} \quad (1)$$

where  $m$  is the vehicle mass,  $I$  is the rotational inertia of the vehicle,  $u$  is the longitudinal speed,  $v$  is the lateral speed,  $\gamma$  is the yaw rate,  $\delta$  is the steering angle of the front wheels,  $B$  is the distance between the left and right wheels on the same axle,  $F_{xij}$  are the longitudinal forces on the wheels, and  $F_{yij}$  are the lateral forces on the wheels.

The vertical forces on the wheels are important factors that have great influences on the output forces of the wheels. The vertical forces of the wheels can be described as follows [17]:

$$\begin{cases} F_{z11} = 0.5mgb / L - 0.5m\dot{u}h / L - 0.5mh(\dot{v} + u\gamma) / B \\ F_{z12} = 0.5mgb / L - 0.5m\dot{u}h / L + 0.5mh(\dot{v} + u\gamma) / B \\ F_{z21} = 0.5mga / L + 0.5m\dot{u}h / L - 0.5mh(\dot{v} + u\gamma) / B \\ F_{z22} = 0.5mga / L + 0.5m\dot{u}h / L + 0.5mh(\dot{v} + u\gamma) / B \end{cases} \quad (2)$$

where  $F_{zij}$  is the vertical forces on the wheel,  $L$  is the distance between the front and rear axles,  $a$  is the distance between the front axle and the center of gravity,  $b$  is the distance between the rear axle and the center of gravity,  $h$  is the height of the center of gravity, and  $g$  is the gravitational acceleration.

The rotation of the wheels can be described as follows [18]:

$$T_{ij} - F_{xij}r - F_{rij}r = I_{ij}\omega_{ij}' \quad (i = 1, 2, j = 1, 2) \quad (3)$$

where  $r$  is the radius of the wheel;  $T_{ij}$  is the driving or braking torque on the wheel;  $F_{xij}$  and  $F_{rij}$  are the longitudinal force and rolling resistance on the wheel, respectively;  $I_{ij}$  is the rotational inertia of the wheel, and  $\omega_{ij}$  is the rotational speed of the wheel.

## 2.2. Motor Model

In this paper, two permanent magnet synchronous motors are chosen as the driving motors for the vehicle. The motor is powered by a battery through a DC-DC converter and controlled by the motor control unit. The wheels on front axle are driven by the motors through gearboxes. The power/moment external characteristics of the motor are shown in Figure 3.

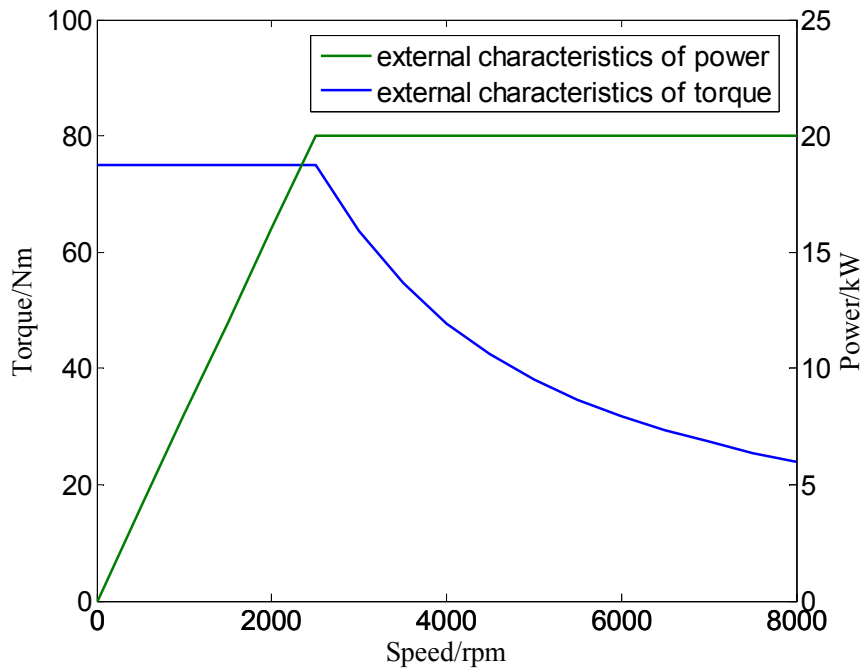


**Figure 3.** Motor power/moment external characteristics.

Because the response of the motor torque is much faster than the dynamic response of the wheel, the dynamic response of the motor can be simplified as a second-order system. The torque command is given by the vehicle controller according to the position of accelerator. Considering the steady error, the motor torque response can be described as follows [19]:

$$T_m(s) = \frac{T_{cmd}(s)(1 + \varepsilon)}{1 + 2\xi s + 2\xi^2 s^2} \tag{4}$$

where  $T_{cmd}$  is the torque command which should be smaller than the maximum torque of the motor,  $\xi$  is the parameter of the dynamic response,  $\varepsilon$  is the steady torque error. A specific motor has its own specific steady output error. According to the test report for a motor for an experimental electric vehicle, the maximum steady error of the torque output can be 5%. Thus, for this vehicle, it is reasonable to assume that the motor on the left side outputs a torque larger than the command value by 5%, and the motor on the right side outputs a torque smaller than the command value by 5%.

The power of the motor can be calculated with the information of motor torque, speed and efficiency. The efficiency of the motor is a function of motor torque and motor speed. The efficiency map of the motor model is given as a 2D lookup table based on the dynamometer tests of the vehicle motor. Therefore the power of the motor can be described as follows [20]:

$$P_m = \begin{cases} T_m \omega_m / \eta_1(T_m, \omega_m) & \text{motoring} \\ T_m \omega_m \eta_2(T_m, \omega_m) & \text{generating} \end{cases} \tag{5}$$

where  $P_m$  is the motor power,  $\omega_m$  is current motor speed, and  $\eta_1$ ,  $\eta_2$  are the motoring efficiency and generating efficiency of the motor which can be obtained from the 2D lookup table with the current motor torque and speed.

2.3. Battery Model

A lithium-ion battery is chosen for the proposed electric vehicle. The voltage of the battery is 180 V and the rated capacity is 55 Ah. The equivalent circuit model has been widely used to describe the characteristics of lithium-ion battery for electric vehicle [21]. Figure 4 shows the equivalent circuit battery model for the proposed vehicle model.  $E_m$  and  $R_0$  are the open circuit voltage and internal resistance. Two pairs of RC circuits  $R_1, C_1$  and  $R_2, C_2$  are used to describe the dynamic process of the battery. Each of the elements is a function of state-of-charge (SOC) and can be obtained through tests.  $U_0$  and  $I_0$  are the output voltage and current. The electric behavior of the circuit can be described as follows [21]:

$$\begin{cases} \frac{du_1}{dt} = -\frac{1}{R_1 C_1} u_1 + \frac{1}{C_1} I_0 \\ \frac{du_2}{dt} = -\frac{1}{R_2 C_2} u_2 + \frac{1}{C_2} I_0 \\ E_m = u_1 + u_2 + I_0 R_0 + U_0 \\ P_0 = U_0 I_0 \end{cases} \quad (6)$$

where  $P_0$  is the output power of the battery which is equal to  $P_m$ , and  $u_1, u_2$  are the voltages of  $R_1, R_2$ .

The SOC of the battery can be described as follows [21]:

$$SOC = SOC_{init} - \frac{1}{C_N} \int_{t_0}^t I_0 dt \quad (7)$$

where  $SOC_{init}$  is the initial SOC and  $C_N$  is rated capacity of the battery.

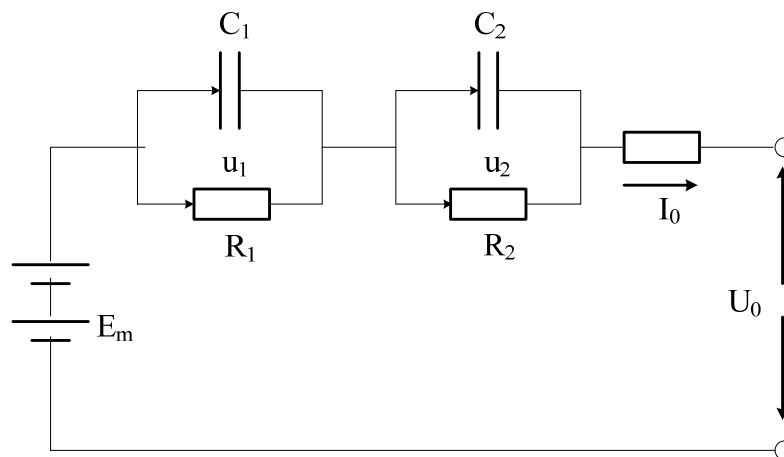


Figure 4. The equivalent circuit battery model.

2.4. Tire Model

The tire model is described using the Magic Formula, which was proposed by Pacejka *et al.* [22] and widely used to describe the dynamic characteristics of tires. The Magic Formula employs combinations of trigonometric functions to precisely describe the tire forces. The tire forces are mainly determined by the slip ratio of the wheel, vertical load of the tire, and slip angle of the tire.

Under a no-steering driving condition, the longitudinal force of the wheel can be described as follows [22]:

$$\begin{cases} F_{x0} = D_1 \sin\{C_1 \arctan[B_1\lambda - E_1(B_1\lambda - \arctan B_1\lambda)]\} \\ \lambda = \frac{\omega r - u}{\omega r} \\ D_1 = a_1 F_z^2 + a_2 F_z \\ C_1 = a_0 \\ B_1 = \frac{a_3 F_z^2 + a_4 F_z}{C_1 D_1 \exp(a_5 F_z)} \\ E_1 = a_6 F_z^2 + a_7 F_z + a_8 \end{cases} \quad (8)$$

where  $F_{x0}$  is the longitudinal force;  $\lambda$  is the slip ratio; and  $a_i$  are the fitting coefficients.

Under a steering condition without a driving or braking force, the lateral force of the tire can be described as follows [22]:

$$\begin{cases} F_{y0} = D_2 \sin\{C_2 \arctan[B_2x - E_2(B_2x - \arctan B_2x)]\} + \Delta S_v \\ x = \alpha + \Delta S_h \\ D_2 = b_1 F_z^2 + b_2 F_z \\ C_2 = b_0 \\ B_2 = \frac{b_3 \sin(b_4 \arctan(b_5 F_z))(1 - b_{12} |\theta|)}{C_2 D_2} \\ E_2 = b_6 F_z^2 + b_7 F_z + b_8 \\ \Delta S_h = b_9 \theta \\ \Delta S_v = (b_{10} F_z^2 + b_{11} F_z) \theta \end{cases} \quad (9)$$

where  $F_{y0}$  is the lateral force;  $\alpha$  is the slip angle of the tire and  $\theta$  is the camber of the tire;  $\Delta S_v$  and  $\Delta S_h$  are compensating factors of the tire; and  $b_i$  are the fitting coefficients.

By combining Equations 8 and 9, the longitudinal and lateral forces under normal driving conditions can be described as follows:

$$\begin{cases} F_x = \frac{\sigma_x}{\sigma} F_{x0}, \quad F_y = \frac{\sigma_y}{\sigma} F_{y0} \\ \sigma = \sqrt{\sigma_x^2 + \sigma_y^2}, \quad \sigma_x = \frac{|\lambda|}{1 + |\lambda|}, \quad \sigma_y = \frac{|\tan \alpha|}{1 + |\lambda|} \end{cases} \quad (10)$$

where  $F_x$  is the longitudinal force of the tire and  $F_y$  is the lateral force of the tire.

The fitting coefficients of the model can be obtained from experiment results of tire tests and are listed in Table 2 [23].

**Table 2.** Fitting coefficients of the Magic Formula.

No.	1	2	3	4	5	6	7	8				
$a_i$	-21.3	1144	49.6	226	0.069	-0.006	0.056	0.486				
No.	1	2	3	4	5	6	7	8	9	10	11	12
$b_i$	-22.1	1011	1078	1.82	0.208	0	-0.354	0.707	0.028	0	14.8	1.122

### 3. Acceleration Slip Regulation Control Strategy

#### 3.1. Analysis of Control Tasks

When the vehicle is running on a low friction road, if the driving torque exceeds the maximum torque provided by the road, the driving wheels will experience excessive spin. This excessive spin of the driving wheels will lead to a decrease in the longitudinal driving force and lateral stability of the vehicle, so it is necessary to prevent the excessive spin of the driving wheels. Because the longitudinal force is mainly affected by the slip ratio, directly controlling the slip ratio is an effective and widely used way to achieve better acceleration performance. To obtain the slip ratio of the driving wheels, it's necessary to measure the rotational speed of the driving wheels and the speed of the vehicle. The speed of each wheel can be measured by wheel speed sensor and the speed of the vehicle can be calculated out by the speed of driven wheels.

For the distributed drive electric vehicle described in this paper, the torque response characteristics of the independent motors are different, and the output torque difference between the left and right will result in a yaw moment. This yaw moment will generate a yaw rate and make the vehicle ran out of the driving lane during straight line driving. The steady errors of the motors were discussed in Section 2. Simulation results using the previously described model showed that a yaw rate of 0.005 rad/s would be generated during a certain acceleration slip regulation process. This yaw rate would lead to a 3 m lateral movement over a straight line driving distance of 50 m, which is unsafe for the vehicle. The experimental results of Akiba *et al.* [15] showed that for the acceleration slip regulation control of a distributed drive electric vehicle, because of the output difference between the two sides, an additional steering wheel angle is needed to keep the vehicle running straight. Direct yaw moment control based on motor torque control is an advantage for distributed drive electric vehicle, so the yaw rate of the vehicle can be controlled by the driving motors instead of adding additional steering operation by the driver. Based on the analysis above, the tasks of the control strategy proposed in this paper will include slip ratio control and yaw rate control.

#### 3.2. Slip Ratio Control

##### 3.2.1. Target Slip Ratio for Acceleration Slip Regulation

The goal of the slip ratio control is to make full use of the road grip. Therefore, it is necessary to obtain the optimal slip ratio that can produce the maximum longitudinal driving force. Under different road conditions, the relationships between normalized driving force  $\mu = F_x/F_z$  and slip ratio  $\lambda$  are different. The  $\mu$ - $\lambda$  Function given by Burckhardt can be used to described the characteristics of typical road conditions [24]:

$$\mu(\lambda) = c_1(1 - e^{-c_2\lambda}) - c_3\lambda \quad (11)$$

The fitting coefficients, optimal slip ratios and the maximum driving forces of six typical road conditions, including dry asphalt, wet asphalt, dry cement, wet cobblestone, snowy and icy, are listed in Table 3. The  $\mu$ - $\lambda$  curves are shown in Figure 5.

**Table 3.** Fitting coefficients and parameters of Burckhardt Model.

No.	Road condition	C1	C2	C3	$\lambda_{opt}$	$\mu(\lambda_{opt})$	$\mu(\lambda_0)/\mu(\lambda_{opt})$
1	Dry asphalt	1.2801	23.990	0.5200	0.17	1.1700	99.74%
2	Wet asphalt	0.8570	33.822	0.3470	0.13	0.8013	99.79%
3	Dry cement	1.1973	25.168	0.5373	0.16	1.0900	99.91%
4	Wet cobblestone	0.4004	33.708	0.1204	0.14	0.3800	99.95%
5	Snowy	0.1946	94.129	0.0646	0.06	0.1906	97.01%
6	Icy	0.0500	306.39	0.0010	0.03	0.0500	99.7%

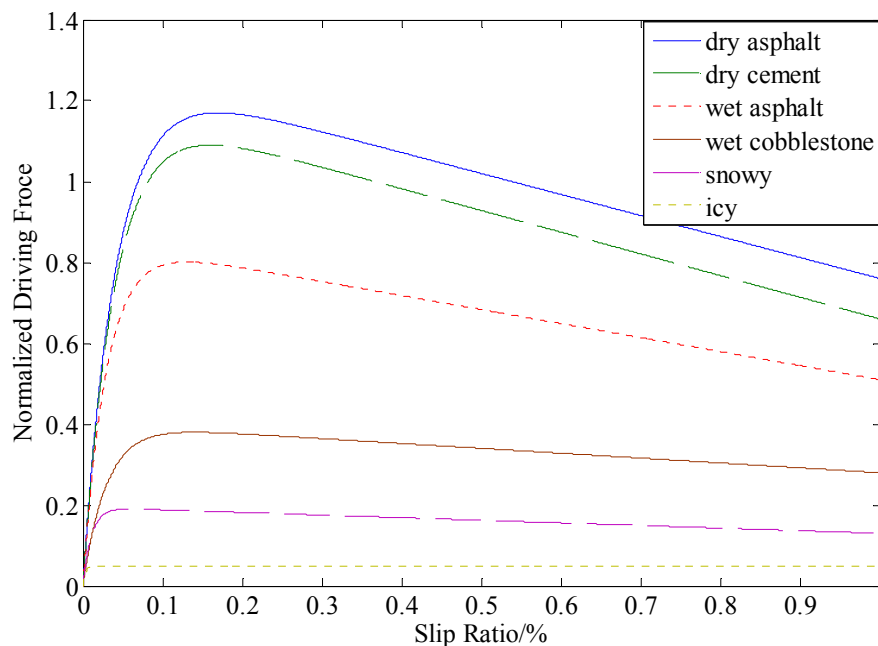


**Figure 5.**  $\mu$ - $\lambda$  curves of standard road conditions.

Under different road conditions, the optimal slip ratio  $\lambda_{opt}$  varies from 3% to 17%. In order to make full use of road friction, the optimal slip ratio should be set according to the road conditions. Typical methods use the information of the current  $\mu$  and  $\lambda$  to match the standard  $\mu$ - $\lambda$  curves and find out the most similar one. However when the road condition is changed during acceleration slip regulation,  $\mu$  and  $\lambda$  will change rapidly. In addition it's not easy to measure  $\mu$  and  $\lambda$  accurately. The measurement error will greatly affect the accuracy of the identification.

In this article, in order to avoid the error during the identification of road condition, a fixed point which is fit for typical road conditions is given. The fixed point  $\lambda_0$  is not the optimal point under most road conditions. However for all conditions,  $\mu(\lambda_0)$  is close to  $\mu(\lambda_{opt})$ , and the average difference under typical road conditions is the smallest. The characteristics of  $\lambda_0$  can be described as follows:

$$\begin{cases} \mu_i(\lambda_0) / \mu_i(\lambda_{opt}) \geq 95\% \\ f(\lambda) = \sum (1 - \mu_i(\lambda) / \mu_i(\lambda_{opt})) \\ f(\lambda_0) = \min f(\lambda) \quad \lambda \in [0,1] \end{cases} \quad (12)$$

The solution of  $\lambda_0$  can be obtained by solving the nonlinear programming problem:

$$\begin{aligned} \min f(\lambda) &= \sum (1 - \mu_i(\lambda) / \mu_i(\lambda_{opt})) \\ \text{st.} & \\ \begin{cases} \mu_i(\lambda_0) / \mu_i(\lambda_{opt}) \geq 95\% \\ \lambda \in [0, 1] \end{cases} & \end{aligned} \tag{13}$$

By using off-line simulation, the solution  $\lambda_0$  can be obtained easily. The answer to the problem is  $\lambda_0 \approx 15\%$ , so 15% is chosen as the fixed point. It can be seen from Table 3 that by keeping the slip ratio of the driving wheel stable at  $\lambda_0$ , the longitudinal road friction can be keep almost the same as the maximum point for all typical road conditions.

### 3.2.2. The Control Method of Slip Ratio

As the target slip ratio for acceleration slip regulation is confirmed, when the slip ratio exceeds the target value, slip ratio control should be activated and keep the slip ratio stable at the target point. Since there is vibration during the slip ratio control, to avoid entering and exiting slip ratio control frequently, the slip ratio control stops when the slip ratio is smaller than  $0.8\lambda_0$  and lasts for five motor torque control cycles,  $c = 50$  ms. The conditions for entering and exiting the acceleration slip regulation can be described as follows:

$$\begin{cases} \text{entering: } \lambda(t) \geq \lambda_0 \\ \text{exiting: } \lambda(x) \leq 0.8\lambda_0, t - c < x \leq t \end{cases} \tag{14}$$

Because the vehicle is driven by the two motors on the front axle, ignoring the wind resistance, rolling resistance and the dynamic response process of the motor torque, the state of a driving wheel can be described as follows [18]:

$$\begin{cases} T_d - F_x r = I_1 \omega' \\ m_{1/2} u' = F_x \\ T_d / ig = T_{cmd} (1 + \varepsilon) \end{cases} \tag{15}$$

where  $T_d$  is the driving torque of the wheel,  $F_x$  is the longitudinal force of the wheel,  $I_1$  is the rotational inertia of the wheel,  $m_{1/2}$  is half of the vehicle mass, and  $ig$  is the transmission ratio.

The rate of the slip ratio change can be derived from Equation (5) and described as follows:

$$\lambda' = \frac{\omega' r (1 - \lambda) - u'}{\omega r} \tag{16}$$

Using Equations (15) and (16), the relationship between the motor torque command and the rate of the slip ratio change can be described as follows:

$$\lambda' = \frac{[T_{cmd} (1 + \varepsilon) ig - m_{1/2} u' r] r (1 - \lambda) - I_1 u'}{I_1 \omega r} \tag{17}$$

Thus, for a target rate of slip ratio change, the target torque required can be derived while ignoring the torque error:

$$T_{tgt} = \frac{1}{i} \left[ m_{1/2} u' r + \frac{(\lambda'_{tgt} \omega r + u') I_1}{r(1-\lambda)} \right] \quad (18)$$

where  $\lambda'_{tgt}$  is the target rate of slip ratio change and  $T_{tgt}$  is the target torque.

The actual rate of the slip ratio change can be obtained by applying the target torque:

$$\lambda' = \lambda'_{tgt} + \delta, \quad \delta = \frac{\varepsilon T_{tgt} (1-\lambda) i g}{I \omega} \quad (19)$$

where  $\delta$  is the error of the output, which can be considered to be a constant because it will not change substantially during a specific slip ratio control process.

A control law for the rate of the slip ratio change is proposed using proportional-integral (PI) control, the relationship between the rate of the slip ratio change and the slip ratio is linear. This control law can be described as follows:

$$\lambda'_{tgt} = k_1 (\lambda_0 - \lambda) + \int k_2 (\lambda_0 - \lambda) dt \quad (20)$$

where  $k_1$  and  $k_2$  are related parameters and  $\lambda_0$  is the target slip ratio.

Using Equations 14, 19 and 20, the actual rate of the slip ratio change under the slip ratio control can be described as follows:

$$\begin{cases} \lambda' = k_1 (\lambda_0 - \lambda) + \int k_2 (\lambda_0 - \lambda) dt + \delta \\ \lambda|_{t=0} = \lambda_0 \end{cases} \quad (21)$$

The transform function of Equation (21) can be described as follows:

$$\lambda(s) = \frac{\lambda_0 s^2 + k_1 \lambda_0 s + \delta s + k_2 \lambda_0}{s^3 + k_1 s^2 + k_2 s} \quad (22)$$

Thus, a steady slip ratio output can be derived as follows:

$$\lim_{t \rightarrow \infty} \lambda(t) = \lim_{s \rightarrow 0} s \lambda(s) = \lambda_0 \quad (23)$$

By applying the proposed control, the slip ratio can be maintained at the target value. To ensure that it is possible to exit the slip ratio control when the driver commands it or the road condition changes, the torque command during slip ratio control cannot exceed the torque command given by the driver. The torque command during slip ratio can be described as follows:

$$T_{slip\_cmd} = \min(T_{tgt}, T_{driv}) \quad (24)$$

where  $T_{slip\_cmd}$  is the torque command for the slip ratio control,  $T_{tgt}$  is the target torque required by the target rate of the slip ratio change, and  $T_{driv}$  is the torque required by the driver.

The communication cycle of the motor control unit is 10 ms, so that the control period of slip ratio control is set to 10 ms to make full use of the rapid motor torque response. In order to ensure that the vehicle can run straightly on split- $\mu$  road conditions, the torque commands for both sides will be kept the same. The target torque should be calculated based on the maximum slip ratio of the driving wheels and applied to all the motors, so the torque command for the driving wheels is a function of the driver commands, vehicle speed and the higher slip ratio of the driving wheels:

$$\begin{cases} T_{slip\_cmd} = f(\lambda_{max}, T_{driv}, u') = \min\left(\frac{1}{i}\left[m_{1/2}u' r + \frac{(\lambda'_{igt}\omega_{max}r + u')I_1}{r(1-\lambda_{max})}\right], T_{driv}\right) \\ \lambda'_{igt} = k_1(\lambda_0 - \lambda_{max}) + \int k_2(\lambda_0 - \lambda_{max})dt, \lambda_{max} = \max(\lambda_1, \lambda_2) \end{cases} \quad (25)$$

### 3.3. Yaw Rate Control

The goal of yaw rate control is to keep the vehicle running straight during straight line driving conditions. The yaw rate is generated by the torque difference between the two sides and affects the straight line driving of the vehicle. By controlling the yaw rate around 0, the vehicle can keep driving straight. As the yaw rate can be controlled by direct yaw moment control, it is possible to control the yaw rate by adding an additional yaw moment using PI control. The yaw moment demand is calculated using the PI feedback of the yaw rate and realized by additional torque compensation. The yaw moment demand and motor torque compensation needed to realize the yaw moment can be described as follows:

$$\begin{cases} \Delta T_{yaw} = -a_1\gamma - \int a_2\gamma \\ \Delta T_{yaw} = \frac{ig\Delta T_l}{r} \frac{B}{2} - \frac{ig\Delta T_r}{r} \frac{B}{2} \end{cases} \quad (26)$$

where  $a_1$  and  $a_2$  are the related parameters;  $\Delta T_{yaw}$  is the yaw moment demand; and  $\Delta T_l$  and  $\Delta T_r$  are the torque compensation on the left and right sides, respectively.

The torque compensation is flexible. Because there are two driving wheels, both the mode with torque compensation on a single wheel and the mode with torque compensation on both wheels are reasonable. The choice can be made to satisfy other control requirements.

The two-wheel mode can be described as follows:

$$\begin{cases} \Delta T_l = \frac{\Delta T_{yaw}r}{igB} \\ \Delta T_r = \frac{-\Delta T_{yaw}r}{igB} \end{cases} \quad (27)$$

The one-wheel mode can be described as follows:

$$\begin{cases} \Delta T_l = \frac{2\Delta T_{yaw}r}{igB} \\ \Delta T_r = 0 \end{cases} \quad or \quad \begin{cases} \Delta T_l = 0 \\ \Delta T_r = \frac{-2\Delta T_{yaw}r}{igB} \end{cases} \quad (28)$$

### 3.4. Coordination Control for Acceleration Slip Regulation

#### 3.4.1. Properties and Coordination Requirement

Under normal driving conditions, only yaw rate control will be working. When the vehicle runs into acceleration slip regulation conditions, both the slip ratio and yaw rate need to be controlled. It's necessary to analyze the properties of slip ratio control and yaw rate control during the acceleration slip regulation. The excessive spin of driving wheels would cause significant loss of longitudinal driving force and lateral stability, while the torque errors of motors are usually not big, so the yaw rate

generated by the motor torque difference is quite small and shouldn't affect the stability of the vehicle. Based on safety considerations, slip ratio control should always be satisfied.

As Equation (25) shows, the torque command of slip ratio control is a function of several factors. Among these factors,  $\lambda_{max}$  might be affected by the yaw rate control. When the torque compensation of yaw rate control is applied to the wheels, the slip ratios of the driving wheels will change and  $\lambda_{max}$  might be affected. This means that the slip ratio command might be affected by yaw rate control, and interactions between the two controls might happen. To avoid the interaction during slip ratio control, it's necessary to ensure that  $\lambda_{max}$  will not be affected by the yaw rate control. If the maximum slip ratio is on a constant side and the yaw rate torque compensation can be applied to the other side,  $\lambda_{max}$  and yaw rate control can be separated. The coordination requirement can be described as follows:

$$\left\{ \begin{array}{l} \lambda_{max} = g(T_{slip\_cmd}) = \lambda_r \\ \lambda_{min} = \lambda_l = f(T_{slip\_cmd} + \Delta T_l) \leq \lambda_{max} \\ \Delta T_{yaw} = \frac{ig\Delta T_l}{r} \frac{B}{2} \end{array} \right. \text{ or } \left\{ \begin{array}{l} \lambda_{max} = g(T_{slip\_cmd}) = \lambda_l \\ \lambda_{min} = \lambda_r = f(T_{slip\_cmd} + \Delta T_r) \leq \lambda_{max} \\ \Delta T_{yaw} = -\frac{ig\Delta T_r}{r} \frac{B}{2} \end{array} \right. \quad (29)$$

### 3.4.2. Adjusting and Stable Stage of Slip Ratio Control

Figure 6 shows the slip ratio control progress without yaw rate compensation. The slip ratio of one wheel will be lower than the other one, due to smaller torque output caused by steady torque error or higher- $\mu$  road condition. Since the drivetrain between the by-wheel motor and the wheel is very simple, the drivetrain can be considered as a rigid system. The rotation of the wheels is mainly affected by the motor and the friction force. From Figure 6 we can see that the variation trends of slip ratio and torque command are almost the same. The torque command changes rapidly according to the change of slip ratio, and then quickly converges to the target point. According to the features of torque command and slip ratio, slip ratio control can be divided into two stages, the adjusting stage and the stable stage. The feature of the stable stage is that both torque command and slip ratio are stable. The judgments can be described as follows:

$$\left\{ \begin{array}{l} 0.95\lambda_0 \leq \overline{\lambda_{max}}(t) \leq 1.05\lambda_0 \\ \frac{1}{10} \sum_{i=1}^{10} \frac{|\lambda_{max}(t-i) - \overline{\lambda_{max}}(t)|}{\overline{\lambda_{max}}(t)} \leq 0.05 \\ \frac{1}{10} \sum_{i=1}^{10} \frac{|T_{slip\_cmd}(t-i) - \overline{T_{slip\_cmd}}(t)|}{\overline{T_{slip\_cmd}}(t)} \leq 0.05 \end{array} \right. , \quad \text{where } \left\{ \begin{array}{l} \overline{\lambda_{max}}(t) = \frac{1}{10} \sum_{i=1}^{10} \lambda_{max}(t-i) \\ \overline{T_{slip\_cmd}}(t) = \frac{1}{10} \sum_{i=1}^{10} T_{slip\_cmd}(t-i) \end{array} \right. \quad (30)$$

where  $\lambda_{max}(t-i)$  is the value of  $\lambda_{max}$  at the time of  $i$  control cycles before the moment  $t$ ,  $T_{slip\_cmd}(t-i)$  is the value of  $T_{slip\_cmd}$  at the time of  $i$  control cycles before the moment  $t$ . When the average  $\lambda_{max}$  is close to the target and the amplitude of  $\lambda_{max}$  is small,  $\lambda_{max}$  can be considered as a stable constant. Meanwhile the amplitude of  $T_{slip\_cmd}$  is small, which means  $T_{slip\_cmd}$  changes slowly can reach an equilibrium state. Since both the input and the output of the slip ratio control system are stable, the slip ratio control can be considered to be in a stable stage.  $S$  is defined as the stable flag here, when the judgments are satisfied,  $S = 1$ , otherwise  $S = 0$ .

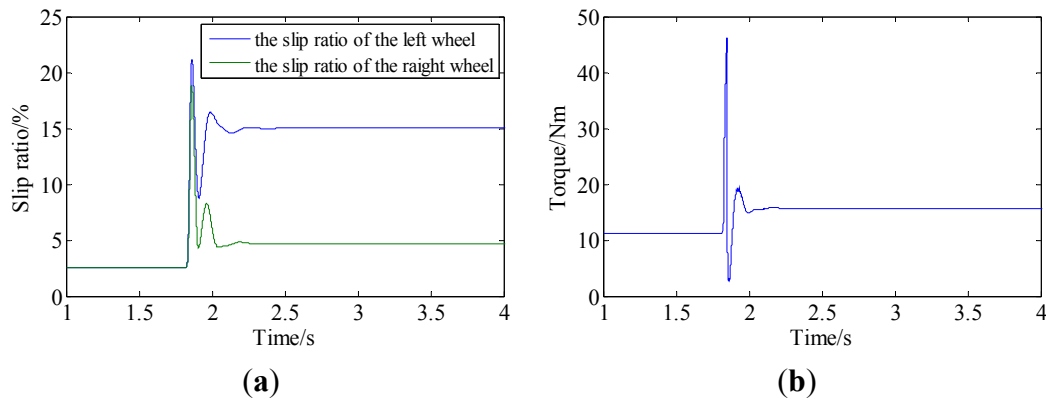


**Figure 6.** Typical slip ratio control progress without yaw rate compensation: (a) slip ratios of both wheels and (b) torque command.

### 3.4.3. The Coordination Control and Implementation

During the adjusting stage, the torque command and the slip ratio change rapidly, and their frequencies are fairly high. In order to satisfy the coordination requirement described by Equation (29),  $\Delta T_{yaw}$  needs to follow the change of  $T_{slip\_cmd}$  and  $\lambda_{max}$ . However, from Equation (26), the calculation of  $\Delta T_{yaw}$  is based on the yaw rate. The frequency of yaw rate is much smaller than the slip ratio as the inertia of the vehicle is much larger than that of the wheels. When  $T_{slip\_cmd}$  and  $\lambda_{max}$  change rapidly, if the lower slip ratio is close to the higher one, then  $\Delta T_{yaw}$  will be requested to change at a high frequency according to Equation (29), but the low frequency prevents  $\Delta T_{yaw}$  from satisfying the high frequency coordination requirement. To avoid this interaction, yaw rate control is not activated during the adjustment stage. The torque commands to both sides are the same as  $T_{slip\_cmd}$ .

When the slip ratio control reaches the stable stage,  $T_{slip\_cmd}$  and  $\lambda_{max}$  can be considered to be constant, and  $\lambda_{min}$  is smaller than  $\lambda_0$ . The control of  $\Delta T_{yaw}$  only needs to satisfy a constant inequality. Setting proper constant boundaries for  $\Delta T_{yaw}$  is a possible solution. According to Equation (29), the slip ratio  $\lambda_{min}$  is only affected by the change of  $\Delta T_{yaw}$ . The slip ratio  $\lambda_{min}$  will gradually increase with the additional torque compensation. To ensure that  $\lambda_{min}$  wouldn't exceed  $\lambda_{max}$ , the addition torque compensation is set as follows:

$$\Delta T_{yaw} = -a_1 \gamma - \int a_2 \gamma$$

$$\begin{bmatrix} a_1 \\ a_2 \end{bmatrix} = \begin{cases} [u_1, u_2]^{-1} & \lambda_{min} \leq 0.95 \lambda_0 \\ [u_1, 0]^{-1} & \lambda_{min} > 0.95 \lambda_0 \end{cases} \quad (31)$$

where  $u_1$  and  $u_2$  are fitting coefficients obtained through experiments. To avoid the situation that  $\Delta T_{yaw}$  is too large when yaw rate control is activated,  $u_1$  should be a small constant. As the slip ratio exceeds  $0.95 \lambda_0$ , the integral coefficient is set to 0, so that  $\Delta T_{yaw}$  will stop increasing, and  $\lambda_{min}$  will stop increasing. Experiment results shows that by using proper fitting coefficients,  $\lambda_{min}$  rarely reaches the threshold. So on the stable stage, the wheel with higher slip ratio is only be controlled by the torque command of slip ratio control and both the torque command of slip ratio control and yaw rate control is added to the wheel with lower slip ratio:

$$\begin{bmatrix} T_{\lambda_{max}} \\ T_{\lambda_{min}} \end{bmatrix} = \begin{bmatrix} 1 & 0 \\ 1 & S \end{bmatrix} \begin{bmatrix} T_{slip\_cmd} \\ K_{yaw} \Delta T_{yaw} \end{bmatrix}, \quad \text{where } K_{yaw} = \begin{cases} 2r / (igB) & \lambda_{min} = \lambda_l \\ -2r / (igB) & \lambda_{min} = \lambda_r \end{cases} \quad (32)$$

Figure 7 shows the implementation of the acceleration slip regulation strategy. The vehicle control unit (VCU) gets the signals of the accelerator, wheel speeds and yaw rate from sensors and then calculates the slip ratio. With the slip ratio information the VCU identifies whether the driving wheels are in an excessive spin state and activates acceleration slip regulation. If the acceleration slip regulation is activated, the slip ratio control will start working, and the motors will be controlled by slip ratio control. If not, the vehicle remains in normal driving conditions. After slip ratio control is activated, the VCU collects information of slip ratios and torque command to judge whether the slip ratio control is in stable stage. If not, only slip ratio control will be applied to the motors. If the slip ratio control reaches the stable stage, yaw control will also be activated and applied to the motor with lower slip ratio.

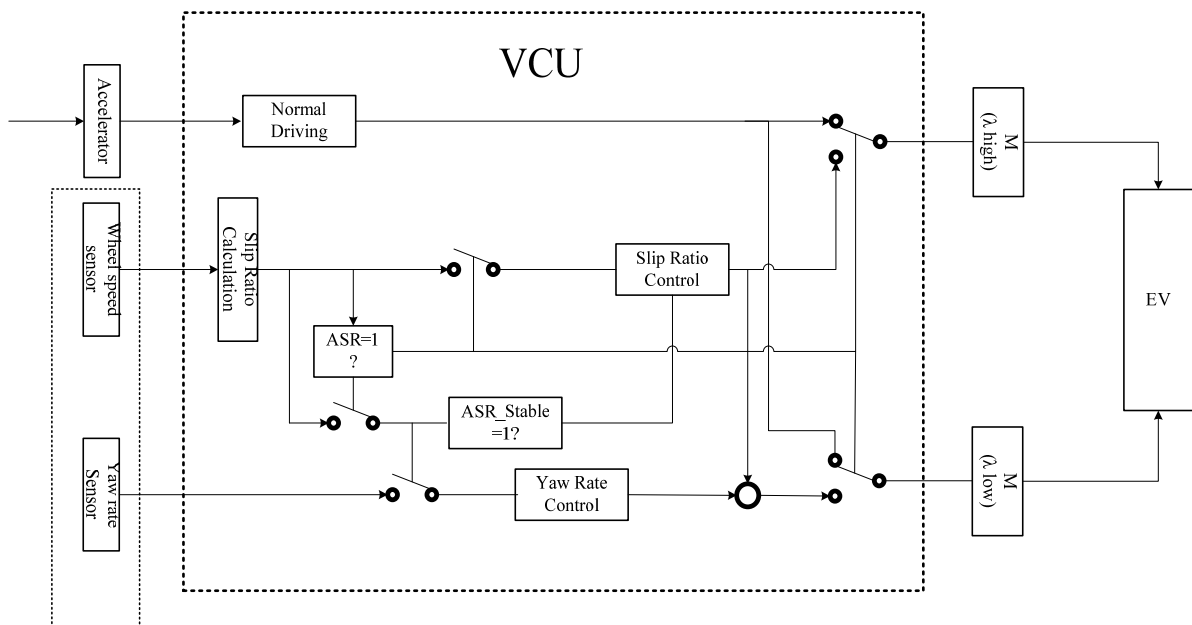


**Figure 7.** Implementation of acceleration slip regulation strategy.

#### 4. Simulation Results and Analysis

The simulation model and parameters of the vehicle and motors were discussed in Section 2. In order to analyze the validity of this strategy, the control effects of the slip ratio and yaw rate will be analyzed. A comparison of the proposed strategy and normal acceleration slip regulation without yaw rate control will also be performed to analyze the advantages of the proposed strategy.

##### 4.1. Simulation of Low Friction Road Conditions

Figure 8 shows the process of acceleration slip regulation on a low friction road. At the beginning, the vehicle was running in a normal driving stage with  $\alpha = 15\%$ . Then at  $t = 1.8$  s,  $\alpha$  was increased to 70% by the driver, the output torque exceeded the maximum friction provided by the road, and excessive spin of the wheels happened. Figure 8a shows that the maximum slip ratio of the driving wheels immediately exceeded the 15% threshold, so acceleration slip regulation was activated. The torque command of the motors followed the slip ratio control, and the maximum slip ratio varied quickly according to the torque command, so that the VCU identified the acceleration slip regulation was at the adjusting stage and yaw rate control was not activated. With slip ratio control, the maximum

slip ratio gradually converged to the target 15%. At  $t = 2.95$  s the VCU identified that the maximum slip ratio and the command  $T_{\text{slip\_cmd}}$  were stable, Figure 8c shows that the vehicle reached the stable stage and the yaw rate control was activated. As shown in Figure 8d, the yaw rate control was applied to the right wheel as its slip ratio was the lowest, and the output torque difference was reduced to almost 0 by the yaw rate control. From Figure 8b, it can be found that the yaw rate was reduced to almost 0. The vehicle finally reached the target stage when no excessive spin of the wheels happened and no yaw rate affecting the straight line driving was generated. The performance of the vehicle reached the control targets.

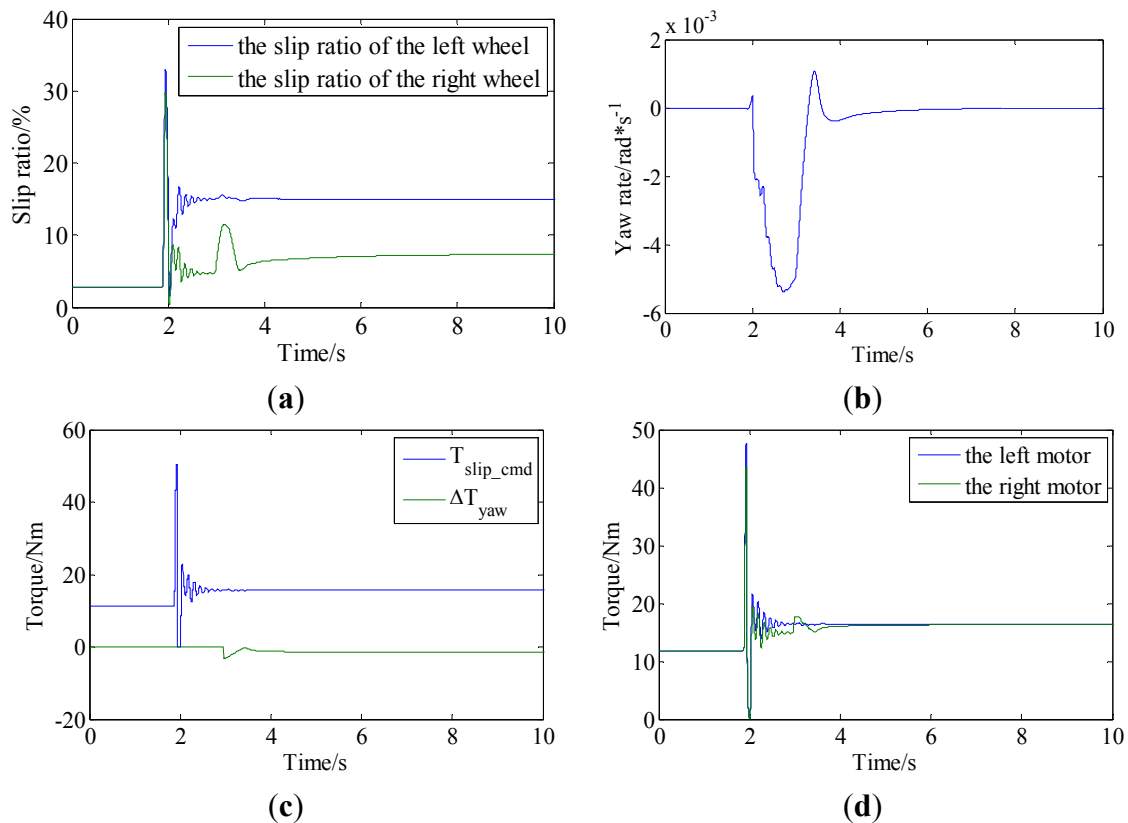


**Figure 8.** Simulation results of acceleration slip regulation on low friction road: (a) slip ratios of driving wheels; (b) yaw rate of vehicle; (c) torque commands of slip ratio control and yaw rate control; and (d) motor torque outputs.

In order to determine the improvement in driving performance provided by the proposed strategy, a simulation of the normal acceleration slip regulation strategy without yaw rate control was also performed for comparison. The driving performance including acceleration and lateral movement are shown in Figure 9. Figure 9a shows the lateral movement of both methods. By applying coordination control with yaw rate control, the lateral movement is reduced from 0.59 m to 0.24 m, so the lateral movement improvement was 59.3%. Figure 9b shows the acceleration performance of the two strategies. The average acceleration was improved by the proposed strategy because of the driving torque compensation. The longitudinal driving force of the driving wheel with the lower slip ratio is enhanced by the torque compensation. The average acceleration improved from  $0.455 \text{ m/s}^2$  to  $0.483 \text{ m/s}^2$ . The average acceleration improvement was 6.1%.

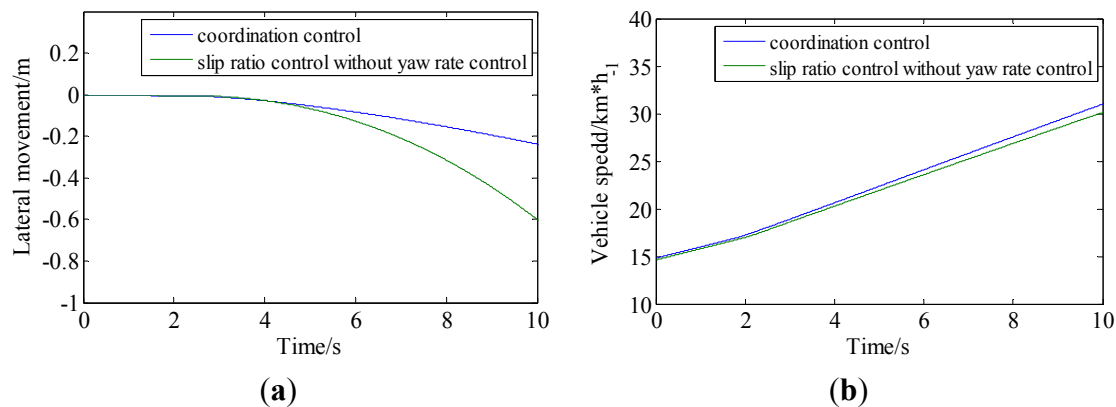


**Figure 9.** Comparison of simulation results of proposed strategy and normal strategy on low friction road: (a) lateral movement and (b) acceleration performance.

From the results listed in Table 4, it's obvious that both the acceleration and straight line driving performance were improved significantly by the proposed strategy.

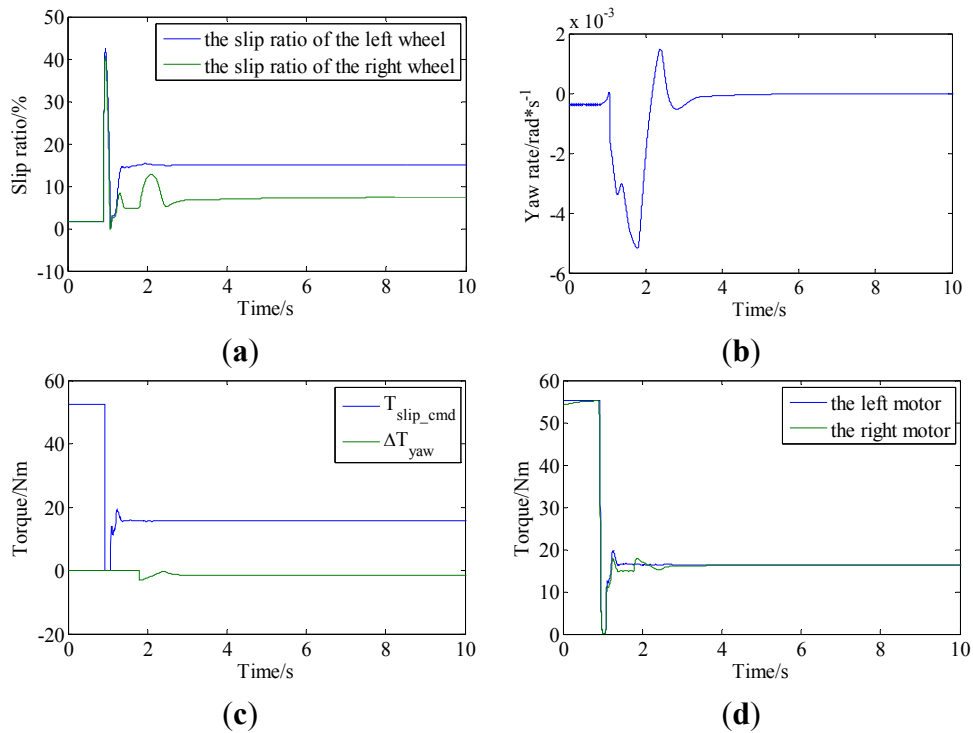
**Table 4.** Performance of acceleration slip regulation on low friction road (simulation).

Performance	Normal strategy	Proposed strategy	Improvement
Average acceleration	0.455 m/s <sup>2</sup>	0.483 m/s <sup>2</sup>	6.1%
Lateral movement	0.59 m	0.24 m	59.3%

#### 4.2. Simulation of Varying Friction Coefficient Road Conditions

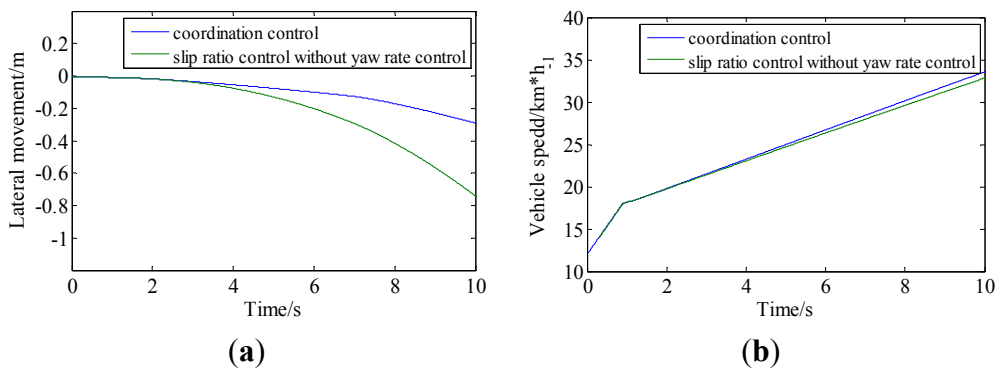
The vehicle was running with a constant accelerator openness  $\alpha = 70\%$ . At the beginning, the friction coefficient of the road was 0.85, and then the friction of the road decreased to 0.1. Under these conditions, the acceleration slip regulation strategy was activated.

Figure 10 shows the working process of acceleration slip regulation. Figure 10a shows the slip ratio conditions of both sides. It can be found that at  $t = 0.9$  s, the friction coefficient decreased to 0.1, so that the torque provided by the motor exceeded the maximum friction of the road, and excessive spin happened on the driving wheels, the maximum slip ratio exceeded the 15% threshold and acceleration slip regulation was activated. The torque commands of the motors followed the slip ratio control. As both slip ratio and torque command were changing rapidly, the VCU confirmed that the vehicle was in the adjustment stage and yaw rate control was not activated. The maximum slip ratio gradually converged to the target 15%. It can be found from Figure 10a,c that at  $t = 1.79$  s the maximum slip ratio and  $T_{\text{slip\_cmd}}$  reached the stable state, The VCU identified that the vehicle was in the stable stage and yaw rate control was activated. As shown in Figure 10d, the yaw rate control was applied to the right side whose slip ratio was lower. During the yaw rate control, the slip ratio of the right side was kept lower than the left, so that the slip ratio control was not affected by the yaw rate control. As it can be found from Figure 10a,b, it is obvious that the slip ratio was under control and the yaw rate was controlled to almost 0. The vehicle achieved the control targets.



**Figure 10.** Simulation results of acceleration slip regulation on a varying friction coefficient road: (a) slip ratios of driving wheels; (b) yaw rate of vehicle; (c) torque commands of slip ratio control and yaw rate control; and (d) motor torque outputs.

A simulation of the normal acceleration slip regulation strategy without yaw rate control was also performed for comparison. The driving performance including acceleration and lateral movement are shown in Figure 11. Figure 11a shows the lateral movement of both methods. By applying coordination control with yaw rate control, the lateral movement is reduced from 0.66 m to 0.26 m, so the lateral movement improvement was 60.6%. Figure 11b shows the acceleration performances of the two strategies. The average acceleration was improved by the proposed strategy because of the driving torque compensation. The longitudinal driving force of the driving wheel with the lower slip ratio is enhanced. As can be seen from the results listed in Table 5, the average acceleration improved from 0.452 m/s<sup>2</sup> to 0.475 m/s<sup>2</sup>. The average acceleration improvement was 5.1%. Both the straight line driving ability and acceleration performance were improved by the proposed strategy.



**Figure 11.** Comparison of simulation results of proposed strategy and normal strategy on variation friction coefficient road: (a) lateral movement and (b) acceleration performance.

**Table 5.** Performance of acceleration slip regulation on variation friction coefficient road (simulation).

Performance	Normal strategy	Proposed strategy	Improvement
Average acceleration	0.452 m/s <sup>2</sup>	0.475 m/s <sup>2</sup>	5.1%
Lateral movement	0.66 m	0.26 m	60.6%

#### 4.3. Simulation of Variation Split- $\mu$ Road Conditions

The vehicle was running with a constant openness of accelerator  $\alpha = 70\%$ . At the beginning, the friction coefficient of the road was 0.85, and then the road condition turned to be a split- $\mu$  road with  $\mu_l = 0.1$  and  $\mu_r = 0.85$ . After a period of time, the road conditions changed to the opposite split- $\mu$  road with  $\mu_l = 0.85$  and  $\mu_r = 0.1$ .

Figure 12 shows the working process of acceleration slip regulation. Figure 12a shows the slip ratio condition of both sides. It can be found that at  $t = 1.1$  s, the vehicle ran into the split- $\mu$  road, the friction coefficient of the left decreased to 0.1, the torque provided by the left motor exceed the maximum friction of the road, excessive spin happened to the left driving wheel, the slip ratio of the left wheel exceeded the threshold 15% and acceleration slip regulation was activated. Though there was no excessive spin on the right wheel, the torque command of the right motor was kept the same as the left to keep the vehicle running straight. The slip ratio of the left wheel gradually converged to the target 15%, and the vehicle reached a stable stage. Figure 12c,d show that at  $t = 1.8$  s the yaw rate control was activated and applied to the right wheel. The yaw rate was gradually controlled to almost zero. Then at  $t = 6.9$  s the vehicle suddenly ran into an opposite split- $\mu$  road with  $\mu_l = 0.85$  and  $\mu_r = 1$ . Then the slip ratios of both wheel changed significantly, and the VCU identified that the vehicle jumped to the adjustment stage, the yaw rate control was exited and only the slip ratio control left. Excessive spin happened to the right wheel, requiring slip ratio control. The control of the left wheel was kept the same as the right side though no excessive spin happened. With slip ratio control, the maximum slip ratio gradually reached the target 15% and the vehicle reached the stable stage again. Figure 12c,d show that at  $t = 7.6$  s the yaw rate control was activated and applied to the left wheel. The yaw rate was controlled to almost zero again. The simulation results show that the strategy can work under complicated road conditions and improve the vehicle performance.

Simulation of the normal acceleration slip regulation strategy without yaw rate control was also performed for comparison. The driving performance including acceleration and lateral movement are shown in Figure 13. Figure 13a shows the lateral movement of both methods. By applying coordination control with yaw rate control, the lateral movement is reduced from 0.74 m to 0.29 m, for a 60.8% improvement of the lateral movement. Figure 13b shows the acceleration performances of the two strategies, where the average accelerations were 0.475 m/s<sup>2</sup> and 0.484 m/s<sup>2</sup>. Due to the application of yaw rate control, the total driving torque was increased on the first split- $\mu$  road and decreased on the second split- $\mu$  road. Whether the acceleration increases or decreases on a split- $\mu$  road depends on the fact that the wheel motor on the low friction side outputs a larger or a smaller torque of the two motors under the same command. Though the average accelerations were given in Table 6, the comparison is useless. Unlike low friction road conditions, the average acceleration of a split- $\mu$  road depends on the

conditions of the road and the motor. However, the lateral movement was greatly decreased, and the straight line driving ability was improved significantly under split- $\mu$  road conditions.

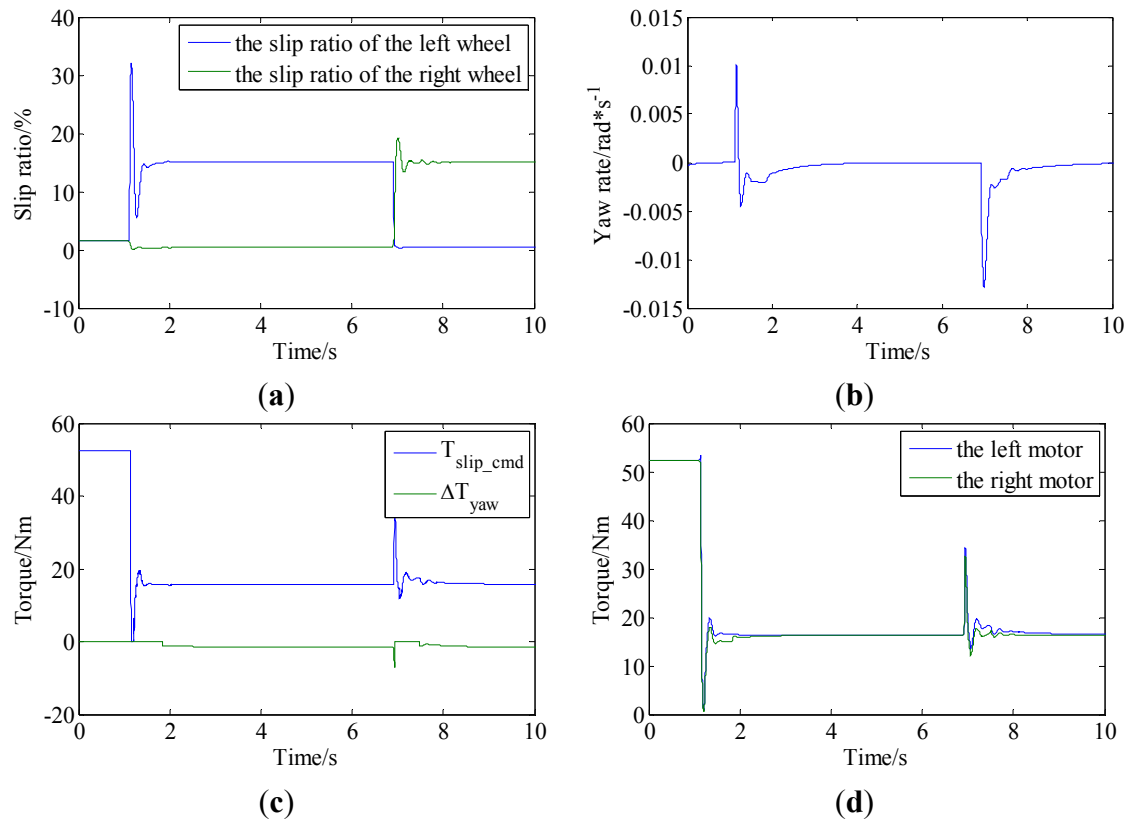


**Figure 12.** Simulation results of acceleration slip regulation on variation split- $\mu$  road: (a) slip ratios of driving wheels; (b) yaw rate of vehicle; (c) torque commands of slip ratio control and yaw rate control; and (d) motor torque outputs.

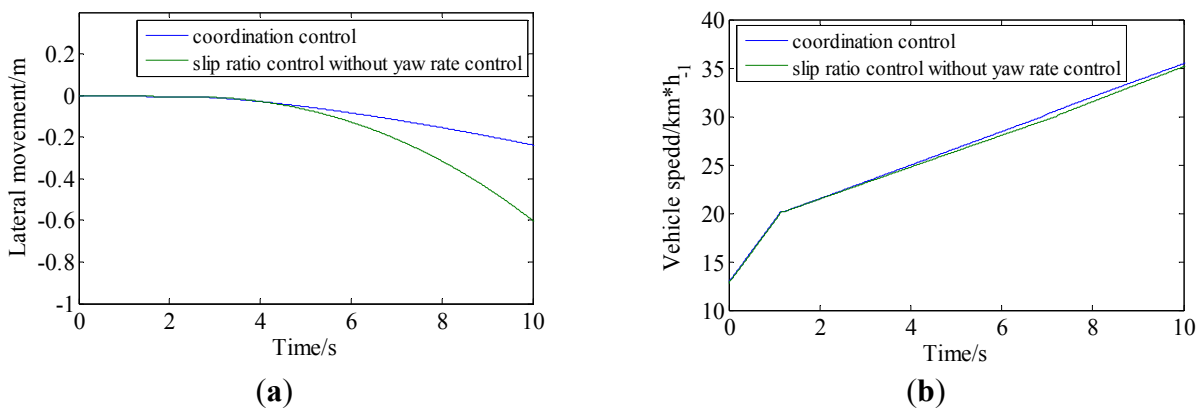


**Figure 13.** Comparison of simulation results of proposed strategy and normal strategy on variation split- $\mu$  road: (a) lateral movement and (b) acceleration performance.

**Table 6.** Driving performance comparison on variation split- $\mu$  road (simulation).

Performance	Normal strategy	Proposed strategy	Improvement
Average acceleration	0.475 m/s <sup>2</sup>	0.484 m/s <sup>2</sup>	1.9%
Lateral movement	0.74 m	0.29 m	60.8%

## 5. Experimental Results and Analysis

### 5.1. Hardware-in-Loop Test Bench

Because the actual motor torque response is much more complicated than the simulation model, a hardware-in-loop test bench was constructed to test whether the control methods could work with real torque responses. In order to obtain the characteristics of actual torque response for real-time simulation, the bench used actual motors to simulate the vehicle motor. Figure 14 shows the structure of the test bench, which included a motor bench, real-time simulation system, and vehicle control unit (VCU). These subsystems were connected by a controller area network (CAN). Information can be transmitted from one subsystem to the other through the CAN.

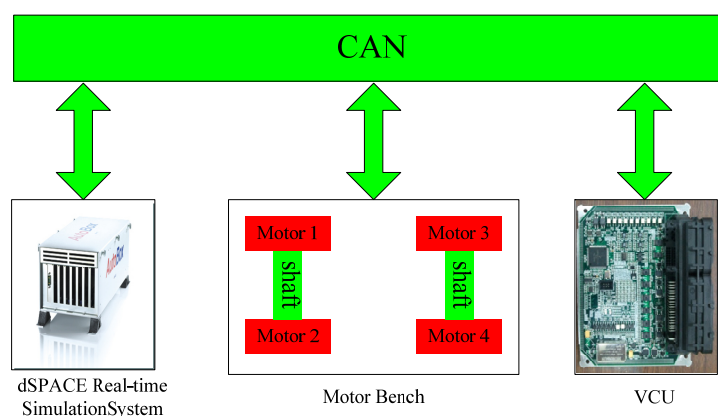


**Figure 14.** Structure of the test bench.

The motor bench used two pairs of motors to simulate two driving motors of a distributed driving electric vehicle. Figure 15 shows the layout of the motor bench. In each pair of motors, one would be used to simulate the vehicle motor, and the other would be used to simulate the load of the vehicle motor. The two motors were connected by a rigid shaft. A sensor was installed on the shaft to measure the rotate speed of the shaft and the output torque which was used to simulate the output torque of the driving motor. The characteristics of the bench motors and accuracy of the measurements for the bench are shown in Table 7.



**Figure 15.** Layout of the motor bench.

**Table 7.** Parameters of the bench motor and measurement accuracy of the bench.

Motor parameters	Rated power	10 kW
	Maximum speed	4,000 rpm
	Rated torque	76.4 Nm
	Torque control accuracy	>99%
	Torque responsive time	20 ms
Measurement accuracy	Torque	0.2%
	Rotate speed	0.5 r/min
	Sample frequency	2 ms

The dSPACE real-time simulation system can receive real-time inputs such as I/O signals, analog signals, and CAN messages from other subsystems and send out real-time outputs in the form of I/O signals, analog signals or CAN messages to other subsystems. Thus, the vehicle dynamic model and the battery model could be built as the simulation model while the real-time motor model could be built with the signals of the motor bench. As the bench motor would be different from the motors of different vehicle models, the bench motor could not be considered as the vehicle motor directly and a real-time simulation model of the vehicle motor should be built based on the real-time information of the bench motors. The relationship between the torque of the bench motor  $T_b$  which was measured by the sensor, and the torque of the motor model  $T_{model}$  which was the output motor torque to vehicle dynamic model, was set to be  $T_{model} = i_1 T_b$ . In order to simulate the load of the vehicle motor, the relationship between the speed of the bench motor  $\omega_b$  and the speed of the motor model  $\omega_{model}$  was set to be  $\omega_{model} = i_2 \omega_b$ . Though the bench motor was not exactly the same as the model, however the dynamic characteristics of actual motor torque response could be reserved for the real-time simulation system. Since the torque control error of the motor control unit is less than 1%, the motor torque  $T_m$  could be considered  $T_m \approx T_{vcu}$ . The steady error  $\varepsilon$  described in Section 2 was the error between the command  $T_{cmd}$  and the output  $T_m$ , and it could be simulated by setting  $T_{vcu} = (1+\varepsilon)T_{cmd}$ . For the simulation of the proposed vehicle model, the coefficients were  $i_1 = 1$  and  $i_2 = 0.5$ , and the steady errors of the motors were set to be the same as the description of the model.

The vehicle controller acted as an actual control unit to control the vehicle dynamic model. The control unit collected the real-time signals from the sensors, vehicle dynamic model, and motor so that it could ran the control strategies to control the bench motor to simulate the driving motor and the load.

By connecting these subsystems together, the test bench could simulate a distributed electric vehicle with real-time control. The proposed strategy could be tested on this bench to verify the validity when applied to complicated actual motors.

## 5.2. Experiment Results and Analysis

### 5.2.1. Hardware-in-Loop Experiment of a Low Friction Road

The conditions of the experiment are almost the same as the simulation. The vehicle was running on a low friction coefficient road and the openness of the accelerator varied from 15% to 70%. Figure 16 shows the results of the experiment. Figure 16a shows that the vehicle ran into the low friction coefficient road at  $t = 11.8$  s, excessive spin happened to the wheels and the slip ratio of the driving

wheels exceeded the 15% threshold, so that acceleration slip regulation is activated. At  $t = 13$  s, the maximum slip ratio was stable around the target, VCU identified that the vehicle was in the stable stage. Figure 16c,d show that yaw rate control was activated at  $t = 13$  s and applied to the right motor. Though the torque compensation caused vibration of the slip ratio of the right wheel, by the proposed yaw rate control method, the slip ratio of the right wheel kept smaller than the left one. No interaction between the two controllers happened. With the slip ratio control and yaw rate control, the vehicle maintained the target slip ratio and kept the yaw rate almost at zero.

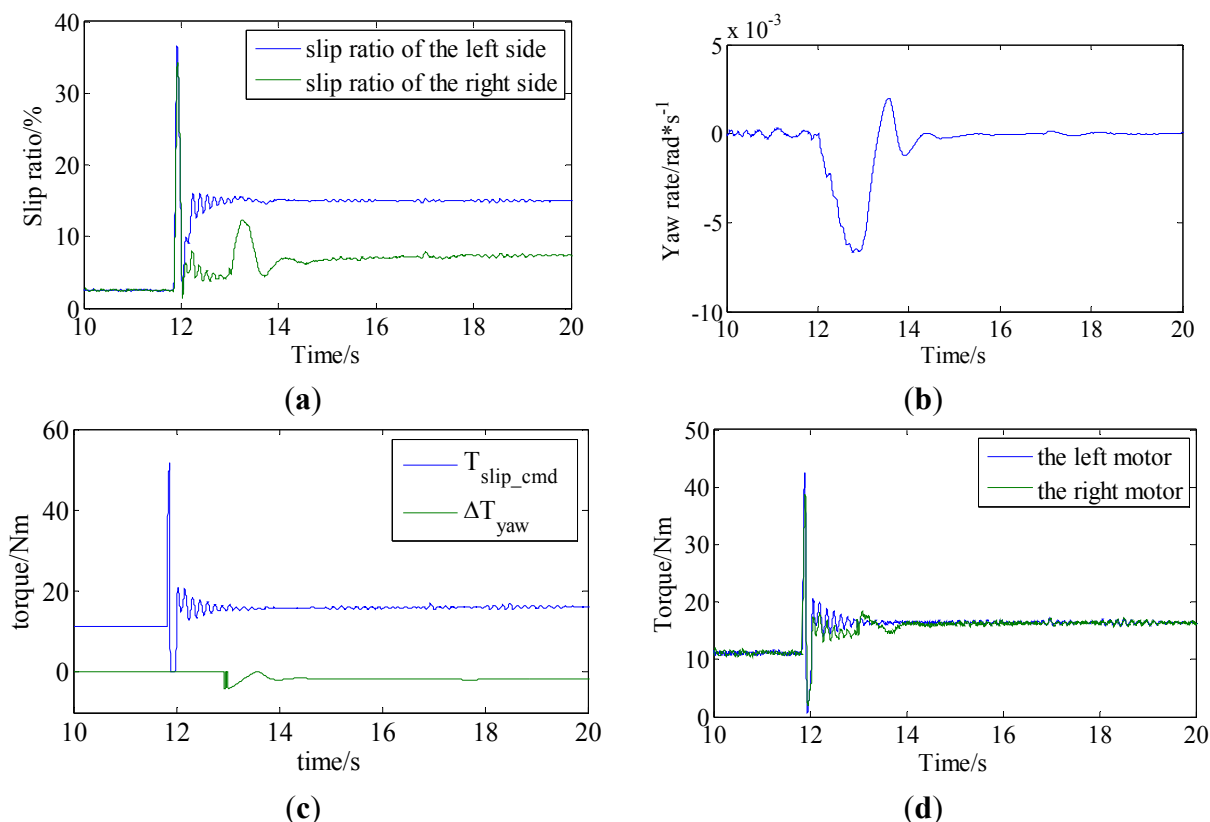


**Figure 16.** Experiment results of acceleration slip regulation on a low friction coefficient road: (a) slip ratios of driving wheels; (b) yaw rate of vehicle; (c) torque commands of slip ratio control and yaw rate control; and (d) motor torque outputs.

As the actual motor torque output was affected by factors like inertia of the motor and the drivetrain damping, it wasn't as ideal as the model, so motor output vibration existed. However, the experimental results showed that it wouldn't affect the effectiveness of the strategy. The results showed that the simulation process is very similar to the experiment, which can serve to prove the effectiveness of the simulation.

A comparison of the results of the proposed strategy and normal acceleration slip regulation strategy is shown in Figure 17. Figure 17a shows the lateral movement of both methods. By applying coordination control with yaw rate control, the lateral movement is reduced from 0.63 m to 0.26 m, so the lateral movement improvement was 58.7%. Figure 17b shows the acceleration performances of the two strategies. Due to the application of yaw rate control, the total driving torque was increased as the driving torque on the lower slip ratio side was increased. As can be seen from the results listed in Table 8, the average acceleration improved from  $0.441 \text{ m/s}^2$  to  $0.473 \text{ m/s}^2$ , and the average

acceleration improvement was 7.3%. Both the acceleration performance and the straight line driving performance were improved.

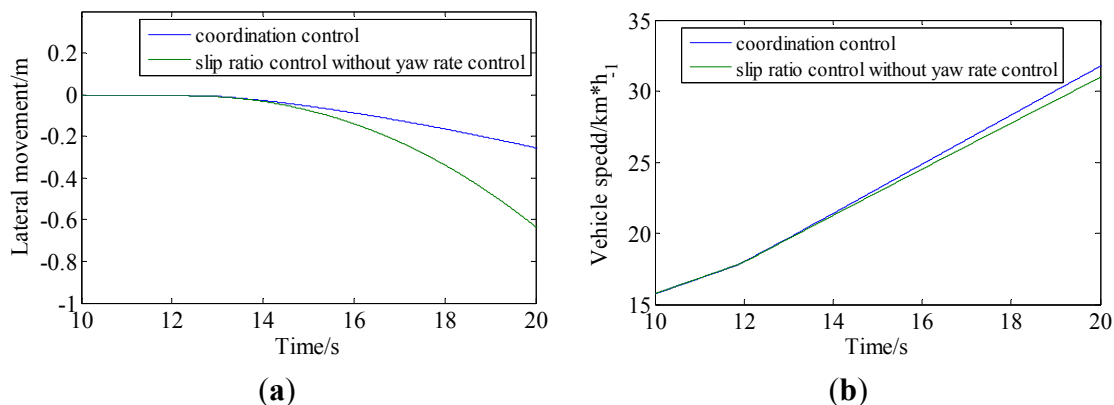


**Figure 17.** Comparison of experiment results of the proposed strategy and normal strategy on a low friction road: (a) lateral movement and (b) acceleration performance.

**Table 8.** Performance of acceleration slip regulation on a low friction road (experiment).

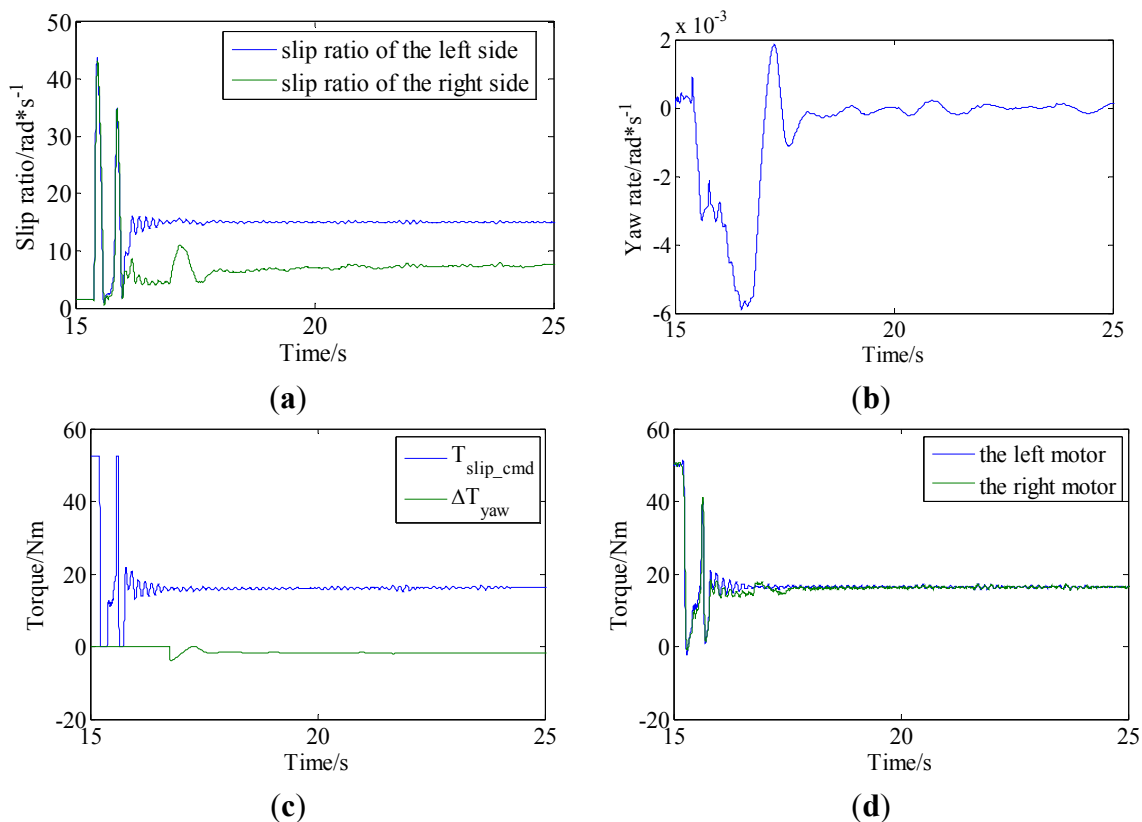
Performance	Normal strategy	Proposed strategy	Improvement
Average acceleration	0.441 m/s <sup>2</sup>	0.473 m/s <sup>2</sup>	7.3%
Lateral movement	0.63 m	0.26 m	58.7%

### 5.2.2. Hardware-in-Loop Experiment of Varying Friction Coefficient Road Conditions

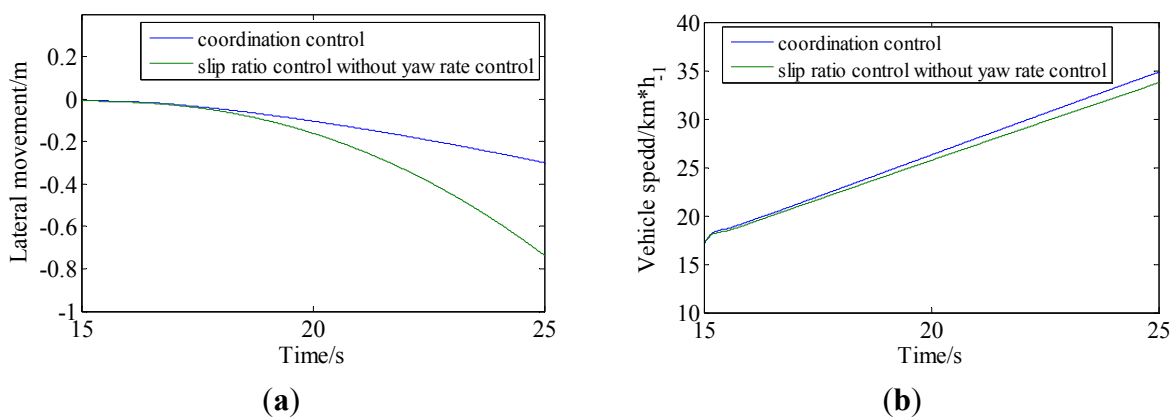
The conditions are described as follows: the vehicle was running with a constant openness of accelerator  $\alpha = 70\%$ . At the beginning, the friction coefficient of the road was 0.85, and then the friction of the road decreased to 0.1. Figure 18 showed the results of the experiment. Figure 18a shows that the vehicle ran into the low friction coefficient road at  $t = 15.3$  s, excessive spin happened to the wheels and the maximum slip ratio exceeded the 15% threshold, and acceleration slip regulation was activated by the VCU. As the VCU identified that the vehicle was in the adjusting stage, yaw rate control was not activated, so that both wheels were under the control of slip ratio control. The maximum slip ratio gradually converged to the target. At  $t = 16.7$  s, the VCU identified that the vehicle was in the stable stage.

Figure 18c,d show that yaw rate control was activated at  $t = 16.7$  s and applied to the right motor. With the coordination control, both maximum slip ratio and yaw rate were under control without interaction between the two controllers. The target of slip ratio control and yaw rate control reached the targets.

A comparison of the experiment results of the proposed strategy and normal acceleration slip regulation strategy is shown in Figure 19. Figure 19a shows the lateral movement of both methods. By applying coordination control with yaw rate control, the lateral movement was reduced from 0.73 m to 0.29 m, so the lateral movement improvement was 60.3%. Figure 19b shows the acceleration performances of the two strategies. The average acceleration improved from 0.453 m/s<sup>2</sup> to 0.475 m/s<sup>2</sup>. The improvement of average acceleration was 5%. The results are listed in Table 9. Judging from the results, the proposed strategy improved the straight line driving performance and the longitudinal acceleration performance for the vehicle during acceleration slip regulation.



**Figure 18.** Experiment results of acceleration slip regulation on variation friction coefficient road: (a) slip ratios of driving wheels; (b) yaw rate of vehicle; (c) torque commands of slip ratio control and yaw rate control; and (d) motor torque outputs.



**Figure 19.** Comparison of experiment results of proposed strategy and normal strategy on variation friction coefficient road: (a) lateral movement and (b) acceleration performance.

**Table 9.** Performance of acceleration slip regulation on variation friction coefficient road (experiment).

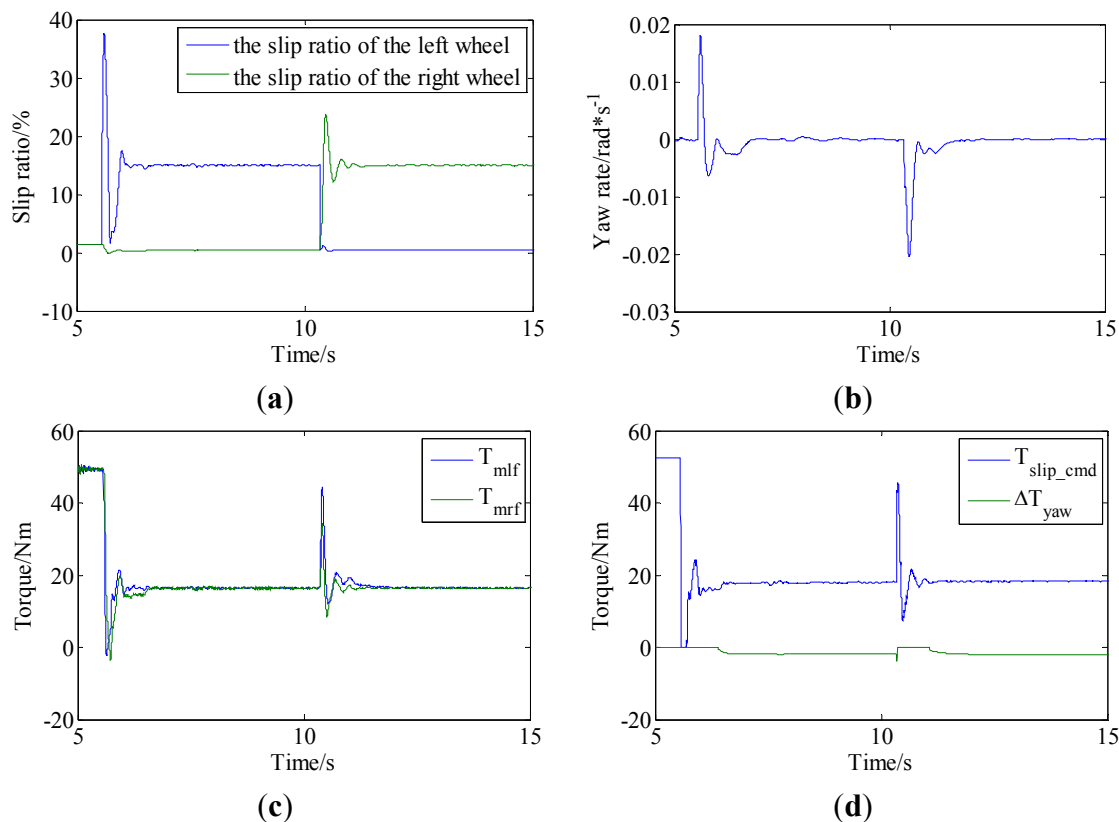
Performance	Normal strategy	Proposed strategy	Improvement
Average acceleration	0.453 m/s <sup>2</sup>	0.475 m/s <sup>2</sup>	5%
Lateral movement	0.73 m	0.29 m	60.3%

### 5.2.3. Hardware-in-Loop Experiment of Varying Split- $\mu$ Road Conditions

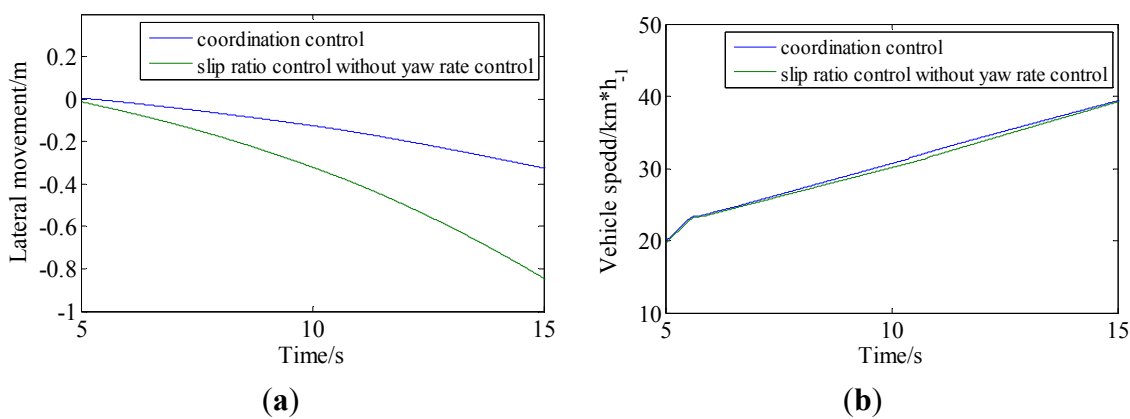
The vehicle was running with a constant openness of accelerator  $\alpha = 70\%$ . The road condition high friction coefficient road varied from  $\mu = 0.85$  to a split- $\mu$  road with  $\mu_l = 0.1$  and  $\mu_r = 0.85$ , and then to the opposite split- $\mu$  road with  $\mu_l = 0.85$  and  $\mu_r = 0.1$ .

Figure 20 shows the working process of the experiment. Figure 20a shows that at  $t = 5.5$  s, the vehicle ran into the split- $\mu$  road, the friction coefficient of the left side decreased to 0.1, on the left side the torque provided by the motor exceeded the maximum friction of the road, and excessive spin happened to the left driving wheel. The slip ratio of the left wheel exceeded the 15% threshold and acceleration slip regulation was activated. During the adjusting stage, both motors were under the control of slip ratio control. The slip ratio of the left wheel gradually converged to the target 15%, and the vehicle reached the stable stage. Figure 20c,d show that at  $t = 6.4$  s the yaw rate control was activated and applied to the right wheel. The yaw rate was gradually controlled to almost zero. Then at  $t = 10.3$  s the vehicle suddenly ran into an opposite split- $\mu$  road with  $\mu_l = 0.85$  and  $\mu_r = 1$ , the slip ratios of both wheels changed significantly, and the VCU identified that the vehicle had jumped to the adjusting stage, the yaw rate control was exited and only the slip ratio control was left. Excessive spin happened to the right wheel and slip ratio control worked. The control of the left wheel was kept the same as the right side as the yaw rate control wasn't activated yet. With slip ratio control, the maximum slip ratio gradually reached the target 15% and became stable. The VCU identified that the vehicle had reached the stable stage of slip ratio control and yaw rate control was activated again. Figure 20c,d show that at  $t = 11.05$  s the yaw rate control was activated again and applied to the left wheel. The yaw rate was gradually controlled to almost zero. The experimental results show that the strategy can work under complicated road conditions, and its effectiveness wouldn't be affected by road condition variations.

Experiments of the normal acceleration slip regulation strategy without yaw rate control were also performed for comparison. The driving performance including acceleration and lateral movement are shown in Figure 21. Figure 21a shows the lateral movement of both methods. By applying coordination control with yaw rate control, the lateral movement was reduced from 0.84 m to 0.32 m, so the lateral movement improvement was 61.8%. Figure 21b shows the acceleration performances of the two strategies. Due to the application of yaw rate control, the total driving torque was increased on the first split- $\mu$  road and decreased on the second split- $\mu$  road. The change of acceleration due to yaw rate compensation depends on the combination of motor characteristics and road conditions on split- $\mu$  road. The acceleration comparison was useless here, however, it could be confirmed from the results listed in Table 10 that the proposed strategy can improved the straight line driving performance without a significant decrease of acceleration under split- $\mu$  road conditions.



**Figure 20.** Experiment results of acceleration slip regulation on variation split- $\mu$  road: (a) slip ratios of driving wheels; (b) yaw rate of vehicle; (c) torque commands of slip ratio control and yaw rate control; and (d) motor torque outputs.



**Figure 21.** Comparison of the experimental results of the proposed strategy and normal strategy on a varying split- $\mu$  road: (a) lateral movement and (b) acceleration performance.

**Table 10.** Driving performance comparison on a varying split- $\mu$  road (experiment).

Performance	Normal strategy	Proposed strategy	Improvement
Average acceleration	0.475 m/s <sup>2</sup>	0.475 m/s <sup>2</sup>	0%
Lateral movement	0.84 m	0.32 m	61.9%

## 6. Conclusions

An acceleration slip regulation strategy for a distributed drive electric vehicle with two motors on the front axle was proposed, based on the coordination of the slip ratio control and yaw rate control. Simulation s and experimental results show the following:

- (1) The proposed slip ratio control method could keep the slip ratio stable at the optimal point when the acceleration slip regulation was activated.
- (2) A yaw rate could be generated by the torque difference between the motors due to the different torque errors, which affects the straight line driving performance. The proposed yaw rate control could reduce the yaw rate and lateral movement.
- (3) The coordination control of the slip ratio control and yaw rate control was proposed, based on an analysis of the priorities and features of the two control processes. The coordination control could prevent the vibration of the control effects.
- (4) Simulations and hardware-in-loop experiments have been carried out under different road conditions, and the effectiveness of the strategy has been verified. Compared with normal acceleration slip regulation, the proposed strategy could improve the acceleration performance on low friction roads and improve the straight line driving performance during the acceleration slip regulation of the vehicle.

## Acknowledgments

This work was supported by the National Natural Science Foundation of China (51475253). The authors would also like to thank the reviewers for their corrections and helpful suggestions.

## Author Contributions

Lingfei Wu constructed the simulation model and designed the control strategy. Lingfei Wu and Jinfang Gou carried out the simulations and experiments. All the authors carried out the data analysis, discussed the results, and contributed to writing the paper.

## Conflicts of Interest

The authors declare no conflict of interest.

## References

1. Nagai, M. The perspectives of research for enhancing active safety based on advanced control technology. *Veh. Syst. Dyn.* **2007**, *45*, 413–431.
2. Chau, K.T.; Chan, C.C.; Liu, C. Overview of permanent-magnet brushless drives for electric and hybrid electric vehicles. *IEEE Trans. Ind. Electron.* **2008**, *55*, 2246–2257.
3. Hori, Y. Future vehicle driven by electricity and control-Research on four-wheel-motored “UOT electric march II”. *IEEE Trans. Ind. Electron.* **2004**, *51*, 954–962.

4. Liu, W.; He, H.; Peng, J. Driving control research for longitudinal dynamics of electric vehicles with independently driven front and rear wheels. *Math. Probl. Eng.* **2013**, *2013*, doi:10.1155/2013/408965.
5. Jalali, K.; Uchida, T.; McPhee, J.; Lambert, S. Development of a fuzzy slip control system for electric vehicles with in-wheel motors. *SAE Int. J. Alt. Power.* **2012**, *1*, 46–64.
6. Gou, J.F.; Zhang, B.; Wang, L.F.; Zhang, J.Z. Acceleration slip regulation of electric vehicles. In Proceedings of the 2010 International Conference on Logistics Engineering and Intelligent Transportation Systems, Wuhan, China, 26–28 November 2010.
7. Zhao, Z. Study of acceleration slip regulation strategy for four wheel drive hybrid electric car. *Chin. J. Mech. Eng.* **2011**, *47*, 83–98.
8. Goran, V.; Karlo, G.; Stjepan, B. Experimental testing of a traction control system with on-line road condition estimation for electric vehicles. In Proceedings of the 21st Mediterranean Conference on Control & Automation (MED), Chania, Crete, Greece, 25–28 June 2013.
9. He, H.; Peng, J.K.; Rui, X.; Hao, F. An acceleration slip regulation strategy for four-wheel drive electric vehicles based on sliding mode control. *Energies* **2014**, *7*, 3748–3763.
10. Lin, C.; Cheng, X.Q. A traction control strategy with an efficiency model in a distributed driving electric vehicle. *Sci. World J.* **2014**, *2014*, doi:10.1155/2014/261085.
11. Yin, G.D.; Wang, S.B.; Jin, X.J. Optimal slip ratio based fuzzy control of acceleration slip regulation for four-wheel independent driving electric vehicles. *Math. Probl. Eng.* **2013**, *2013*, doi:10.1155/2013/410864.
12. Subudhi, B.; Ge, S.S. Sliding-mode-observer-based adaptive slip rate control for electric and hybrid vehicles. *IEEE Trans. Intell. Trans. Syst.* **2012**, *13*, 1617–1626.
13. Yin, D.; Oh, S.; Hori, Y. A novel traction control for EV based on maximum transmissible torque estimation. *IEEE Trans. Ind. Electron.* **2009**, *56*, 2086–2094.
14. Hori, Y.; Toyoda, Y.; Tsuruoka, Y. Traction control of electric vehicle: Basic experimental results using the test EV “UOT electric march”. *Ind. Appl. IEEE Trans.* **1998**, *34*, 1131–1138.
15. Tora, A.; Ryota, S.; Takeshi, F.; Jun, T. A study of novel traction control for electric motor driven vehicle. In Proceedings of the Power Conversion Conference, Nogaya, Japan, 2–5 April 2007.
16. Zhao, Z. Torque adaptive traction control for distributed drive electric vehicle. *Chin. J. Mech. Eng.* **2013**, doi:10.3901/JME.2013.14.106.
17. Gillespie, T. *Fundamentals of Vehicle Dynamic*; SAE Publications: Warrendale, PA, USA, 1992; pp. 8–18.
18. Mirzaeinejad, H.; Mirzaei, M. A novel method for non-linear control of wheel slip in anti-lock braking systems. *Control Eng. Pract.* **2010**, *18*, 918–926.
19. Tahami, F.; Kazemi, R.; Farhanghi, S. A novel driver assist stability system for all-wheel-drive electric vehicles. *IEEE Trans. Veh. Technol.* **2003**, *52*, 683–692.
20. Wang, R.; Chen, Y.; Feng, D.; Huang, X.Y.; Wang, J.M. Development and performance characterization of an electric ground vehicle with independently actuated in-wheel motors. *J. Power Sources* **2011**, *196*, 3962–3971.
21. He, Y.; Liu, X.T.; Zhang, C.B.; Chen, Z.H. A new model for State-of-Charge (SOC) estimation for high-power Li-ion batteries. *Appl. Energy* **2013**, *101*, 808–814.
22. Pacejka, H.B.; Bakker, E. The magic formula tyre model. *Veh. Syst. Dyn.* **1992**, *21*, 1–18.

23. Kong, L. Key Control Technologies Research and Development of Anti-lock Braking System for Industrialization. Ph.D. Thesis, Tsinghua University, Beijing, China, 2006.
24. Harifi, A.; Aghagolzadeh, A.; Alizadeh, G.; Sadeghi, M. Designing a sliding mode controller for slip control of antilock brake systems. *Transp. Res. Part C: Emerg. Technol.* **2008**, *16*, 731–741.

© 2015 by the authors; licensee MDPI, Basel, Switzerland. This article is an open access article distributed under the terms and conditions of the Creative Commons Attribution license (<http://creativecommons.org/licenses/by/4.0/>).